

Simulation of the cosmic ray tau neutrino telescope (CRTNT) experiment

This content has been downloaded from IOPscience. Please scroll down to see the full text.

2009 J. Phys. G: Nucl. Part. Phys. 36 075201

(<http://iopscience.iop.org/0954-3899/36/7/075201>)

View [the table of contents for this issue](#), or go to the [journal homepage](#) for more

Download details:

IP Address: 140.113.38.11

This content was downloaded on 25/04/2014 at 08:33

Please note that [terms and conditions apply](#).

Simulation of the cosmic ray tau neutrino telescope (CRTNT) experiment

J L Liu¹, S S Zhang¹, Z Cao¹, H H He¹, M A Huang², T C Liu³, G Xiao¹, M Zha¹, B K Zhang¹, Y X Bai¹ and Y Zhang¹

¹ Key Laboratory of Astroparticle Physics, Institute of High Energy Physics, Beijing 100049, People's Republic of China

² Department of Energy and Resources, National United University, 1 Lienda, Miao-Li 36003, Taiwan

³ Institute of Physics, National Chiao-Tung University, 1001 Ta-Hsueh Rd, Hsinchu 300, Taiwan

E-mail: liujl@ihep.ac.cn

Received 14 November 2008

Published 1 May 2009

Online at stacks.iop.org/JPhysG/36/075201

Abstract

A τ lepton can be produced in a charged current interaction by a cosmic ray tau neutrino with material inside a mountain. If it escapes from the mountain, it will decay and initiate a shower in the air, which can be detected by an air shower fluorescence/Cherenkov light detector. Designed according to such a principle, the cosmic ray tau neutrino telescope (CRTNT) experiment, located at the foothill of Mt Balikun in Xinjiang, China, will search for very high-energy cosmic τ neutrinos from energetic astrophysical sources by detecting those showers. This paper describes a Monte Carlo simulation for a detection of τ events by the CRTNT experiment. Ultra-high-energy cosmic ray events are also simulated to estimate the potential contamination. With the CRTNT experiment composed of four detector stations, each covering $64^\circ \times 14^\circ$ field of view, the expected event rates are 28.6, 21.9 and 4.7 per year assuming an AGN neutrino flux according to Semikoz and Sigl (2004 *J. Cosmol. Astropart. Phys.* JCAP 04(2004)003), Mannheim–Protheroe–Rachen (MPR) active galactic nucleus (AGN) jet model and Stecker–Done–Salamon–Sommers (SDSS) AGN core model, respectively. Null detection of such a τ event by the CRTNT experiment in 1 year could set a 90% C.L. upper limit on $19.9 \text{ (eV cm}^{-2} \text{ s}^{-1} \text{ sr}^{-1})$ for an E^{-2} neutrino spectrum.

1. Introduction

The origin of cosmic rays (CRs) above 10^{15} eV (1 PeV) has been a long-standing problem. The observation of neutral particles, which can be directly traced back to the sources, is a unique way to search for point sources of CRs under 10^{19} eV. There are many energetic astrophysical sources such as gamma ray bursts (GRBs) or active galactic nuclei (AGNs).

These objects could accelerate particles to ultra-high energy and produce CRs, gamma rays and neutrinos [1, 2]. For photons at 10^{14} – 10^{16} eV, their attenuation length for interaction with cosmological microwave background photons is approximately 10 kpc, roughly the distance from the solar system to the galactic center. Neutrinos are the only choice for exploring remote CR sources. The observation of ultra-high-energy neutrinos is not only an important proof of their existence but also an orthogonal tool, besides conventional astronomical tools such as optical and radio observation, for studying GRBs or AGNs. However, because of very weak interaction, neutrino detection requires a huge volume of the detector medium. A conventional way of neutrino detection is to build or locate a huge volume of target and bury detectors inside so that charged particles as products of interaction between incident neutrinos and target material can be detected. As an example, the IceCube experiment, located near the geographic South Pole in Antarctica, uses natural ice approximately 2 km under the surface as the target and strings of UV-sensitive optical modules buried in the ice to detect Cherenkov light generated by muons and electrons that are produced in the interaction of incident neutrinos [3]. Working in a similar principle, the Antares experiment uses natural water in the Mediterranean Sea instead of ice and sink strings of similar optical modules down to the sea bed to detect Cherenkov photons [4]. The main advantage of underwater/ice neutrino detectors lies in the ability to collect muons from large distances since the muon range is much longer compared to the electron or tau range. For electrons generated by e -neutrino, a cascade in the sensitive area of the detector can be reconstructed. For τ neutrinos in a certain energy range, both the interaction vertex, where the τ lepton is produced, and the τ decay vertex might be present in the sensitive area so that they yield a clear signature of ‘double bang’. Therefore, the detector is sensitive to all species of incident neutrinos with somewhat clear signature for different species. Due to a limited attenuation length of the Cherenkov light, the spacing between optical modules must be sufficiently small in order to collect sufficient Cherenkov photons that enable reasonable reconstruction of tracks or showers inside the detector. This is a disadvantage of this type of detector in terms of costs of construction. It is substantial in the case of neutrino observation with very low statistics, e.g. typically tens of events per year for a scale of experiments such as IceCube. To seek some more economic ways to build larger detectors for statistically significant measurements is in fact essential. Sometimes, one has to sacrifice some performance of the detector to fulfill the goal. One of the many ways to explore economic detection of ultra-high-energy neutrinos is to separate the detector volume from the target volume in which the incident neutrino interacts. By doing so, the target volume can be as large as a piece of mountain or even a part of the earth shell without putting any detector inside, and the detector volume can be as large as the nearby atmosphere, such as that for the HiRes experiment [5] and the Pierre Auger Observatory (PAO) experiment [6]; both are primarily designed for detecting cosmic rays above 1 EeV. An obvious disadvantage is that the interaction vertex is no longer within the scope of the detector. A potential difficulty might be that the observation could be contaminated by the cosmic ray background. There exists a solution to avoid the cosmic ray background by slightly reducing the detector volume with a more dedicated design of configuration that uses the fluorescence/Cherenkov telescopes, such as HiRes/Auger telescopes, to monitor a volume of a few kilometers behind a mountain and keep the field of view (FOV) of these telescopes in the shadow of the mountain. The mountain plays not only the role of a huge target, but also a screen of cosmic rays coming into the field of view of the detector. By mainly collecting the Cherenkov photons, instead of fluorescence photons, generated in air showers, such an array of telescopes can work at energies as low as 1 PeV, the same energy range as the IceCube experiment. This technique is reasonably inexpensive and the detector aperture can be easily increased in scale to compensate for the disadvantage of this technique only effectively detecting tau neutrinos. In the rest of this

paper, we discuss detailed physics perspectives with one of the specific configurations of this type of detector.

Before going into more details, let us briefly review the principle of the detection method. Incident neutrinos convert into electrons, muons and taus in a mountain through the charged current interaction depending upon their flavor. Electrons will shower quickly inside the target material. Muons travel a very long distance before decaying; therefore, they are not easy to be detected using this method. τ leptons produced inside the mountain, which have a sufficiently long lifetime to escape from the mountain, decay and induce showers in the air. A conventional air shower detector, such as fluorescence/Cherenkov telescopes, can then be used to detect them. A cosmic ray tau neutrino telescope (CRTNT) experiment is designed to detect these neutrino-induced air showers [7]. To find a suitable site for the experiment is not trivial because it must be sufficiently dry throughout the year and the mountain must be sufficiently steep so that there is enough space for well-developed showers to be detectable. Strongly depending upon the specific thickness of the mountain and terrain of the site, the CRTNT experiment needs to be re-evaluated for its feasibility with very much updated AGN neutrino models and simulation tools. Since the publication of [7] which addressed the basic principle of the detection, much progress has been made in AMANDAII data analysis, neutrino models and simulation techniques. The purpose of this paper is to address them in detail.

The rest of the paper is organized as follows. The configuration of the CRTNT detector is described in section 2. Section 3 describes in detail the procedure of the τ neutrino converting into the τ lepton in the mountain and detection of the air shower initiated by the τ lepton. In sections 4–6, the event rate and sensitivity of the CRTNT detector are estimated. We summarize all the results for this study and compare them with previous works in section 7.

2. The CRTNT project

The proposed CRTNT project, which currently has two telescopes as a prototype running at the Tibet site [8] and detecting cosmic ray showers observed by the ARGO-YBJ experiment [8], uses fluorescence/Cherenkov light telescopes to detect air showers induced by tau neutrinos. A candidate site is at the foothill of Mt Balikun, about 130 km north of Hami, Xinjiang Province, China. The contour map of the mountain is shown in figure 1. The mountain range runs in the east–west direction and the northern side is quite steep. The height of the mountain stays at about 4000 m a.s.l. for more than 30 km in the east–west direction. At the foothill, the Balikun valley stretches hundreds of kilometers at a height of approximately 1500 m a.s.l. The total precipitation is less than 200 mm per year. The Balikun site provides an excellent convertor for mountain-passing neutrino events and a suitable weather condition for observing the resultant air showers with fluorescence/Cherenkov light telescopes. Preliminarily selected sites for four CRTNT arrays, denoted as FD1, FD2, FD3 and FD4, are located in the northern valley within 30 km from the Balikun city. All sites are convenient in terms of accessibility of power supply and major highways. The ideal orientation of the field of view of the detector enables a decent observation of the galactic center, which is considered as the most favorable neutrino source in our galaxy, with a considerable large exposure. An optimized configuration of the detector array is shown in figure 1.

At each site, four telescopes observe a FOV of 64° in the azimuth angle and 14° in the elevation angle. Each telescope has a mirror of 5 m^2 with a reflectivity of 82%. A focal plane camera consists of 16×16 photomultiplier tubes (PMTs). Each PMT has a hexagonal photo-cathode of 44 mm from side to side with a FOV of approximately $1^\circ \times 1^\circ$. Signals from tubes are read out by 50 MHz flash ADCs to record their complete waveforms. An algorithm for finding the pulse area is used to determine how many photons are detected by each channel.

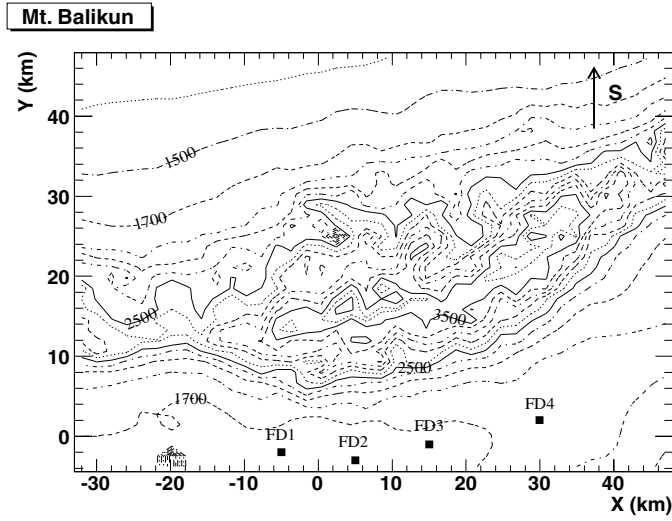


Figure 1. Contour map of Mt Balikun; the numbers represent the altitudes in meter. The solid rectangles are the location of the four CRTNT telescope sites.

A successful triggered event must pass three levels of trigger criteria. The first-level trigger is formed in every single channel, referred to as a tube trigger. It requires the signal-to-noise ratio to be greater than 4σ , where σ is the standard deviation of the total photon–electron noise within a running window of 640 ns. The second-level trigger is formed with coincidence among channels that form certain patterns in the camera, on the basis of a pattern recognition algorithm, referred to as the telescope trigger. The ‘track-type’ pattern requires at least six triggered pixels forming a straight line corresponding to a shower passing through the FOV. The ‘circular-type’ pattern requires seven triggered pixels forming a solid circle corresponding to a Cherenkov image of a shower pointing toward the telescope. The patterns are searched within a 6×6 box running over the entire camera. The third-level trigger for an event requires at least one telescope to be triggered.

3. Monte Carlo simulations

The simulation of a τ neutrino event is divided into the following three stages: (1) the τ neutrino interacts inside the mountain, (2) the τ lepton decays and initiates an air shower and (3) photons are generated from the shower and detected by the CRTNT detector. To estimate the background for the neutrino detection, CR showers flying over the mountain are also generated. Both the fluxes of neutrinos and CRs are assumed to be isotropic and uniform in the FOV of the detector.

3.1. Tau neutrino interaction

Primary neutrinos ranging from 1 PeV to 6 EeV are sampled according to models that predict fluxes from AGNs [9–12]. Incident neutrinos are uniformly distributed from 73° to 101° in the zenith angle and from 0° to 180° in the azimuth angle (the west is defined as 0° in azimuth). All neutrinos enter the mountain from the southern side. A three-dimensional global coordinate system is employed to describe the incident directions, interaction positions of τ neutrinos

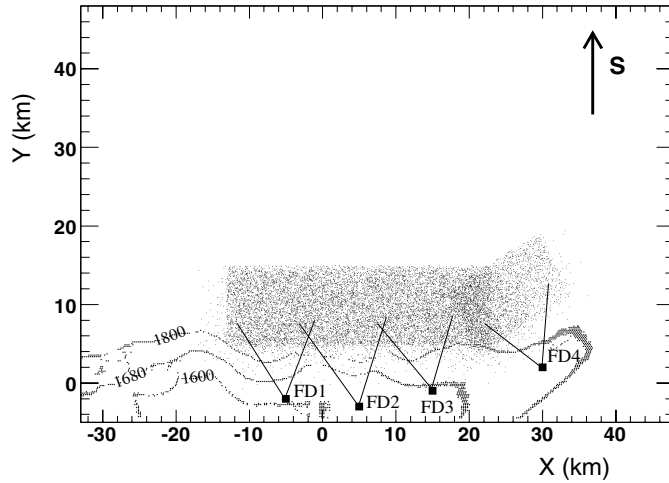


Figure 2. Starting points of showers initiated by τ leptons. The solid rectangles represent four potential CRTNT sites and the touched lines indicate the FOV of telescopes on each site. The dotted curves show the mountain profile near the four sites.

and mountain profile, which are modeled by a digital topological map. A one-dimensional coordinate system along the trajectory is defined to describe all the three stages. If incident ν_τ interacts inside the mountain, the energy and momentum of τ produced are traced until it decays. The energy loss and the decay position of τ are simulated. Regeneration of ν_τ is taken into account, i.e. if τ decays inside the mountain, the decay product ν_τ will be traced by again using the same procedure.

SHINIE (Simulation of High-Energy Neutrinos Interacting with the Earth), a Monte Carlo simulation package, is used to describe the neutrino interaction in our simulation. In this package, the inelasticity y and the differential cross-section $d\sigma/dy$ are calculated separately, using the latest parton distribution function CTEQ6 [13]. The newly calculated cross section below 1 EeV is about 7% less than the result in the package LEPTO [14]. The tau/muon lepton energy loss is also calculated in details. The detailed description can be found in [15] and references therein.

3.2. Tau decay and air shower initiation

Once a τ lepton escapes from the mountain and decays in the air, energies of daughter particles are simulated using TAUOLA [16] for all decay channels. Electrons and hadrons (a branch ratio of 83%) will initiate air showers. The air shower carries approximately one-half of the τ energy. The starting point of the shower along the particle trajectory is calculated according to the random sampling of the τ decay length, while the shower direction is the same as that of the primary ν_τ . The projection of all the starting points is shown in figure 2. If decays occur behind the detector, the shower cannot be detected and is ignored in the simulation.

Corsika (version 6.611) [17] is employed to generate air showers in the space between the shower initiating points and the CRTNT detectors. A pre-simulated shower library is established at 33 selected energies distributed between 0.1 PeV and 0.6 EeV. At each energy, 100 hadronic (pion as the primary particle) and 100 electromagnetic (electron as the primary particle) showers are simulated. The longitudinal profiles of showers, i.e. the number of

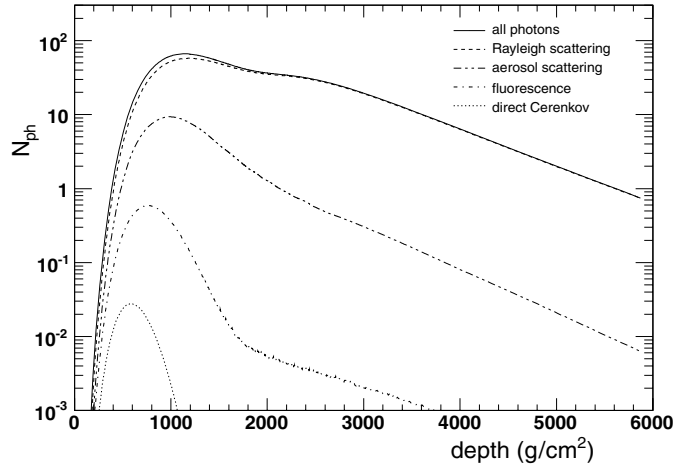


Figure 3. Profiles of all photons seen by the detector along the shower longitudinal development of a typical event. The solid curve is the sum of all photons. The dashed curve is Cherenkov photons scattered by atmospheric molecules (Rayleigh scattering). The double-dot-dashed curve is Cherenkov photons scattered by aerosols. The dot-dashed curve represents fluorescence photons. The dotted curve represents direct Cherenkov components.

charged particles as a function of the slant depth at every 5 g cm^{-2} in the air, are recorded in the library. The depth of air is calculated according to the US standard atmosphere model (1976) [18]. The earth curvature is taken into account.

A shower profile is randomly selected from the library according to the particle identification at the closest energy, and the number of charged particles in a shower is scaled up or down to represent the shower to be simulated.

3.3. Photon production and the CRTNT detector simulation

Ultraviolet fluorescence light is generated as charged shower particles passing through the atmosphere. Laterally, fluorescence photons are assumed to follow a distribution of electrons described by the Nishimura–Kamata–Greisen (NKG) formalism [19]

$$\rho(r) = \frac{N}{(r_0)^2} f\left(s, \frac{r}{r_0}\right). \quad (1)$$

where r_0 is the Moliere unit and s is the age of the shower. The normalized function f reads as

$$f\left(s, \frac{r}{r_0}\right) = \left(\frac{r}{r_0}\right)^{s-2} \left(1 + \frac{r}{r_0}\right)^{s-4.5} \frac{\Gamma(4.5 - s)}{[2\pi\Gamma(s)\Gamma(4.5 - 2s)]}. \quad (2)$$

Cherenkov photons are also generated by charged particles if the particle energy is higher than the threshold energy. Photons scattered by the atmospheric molecules and aerosols are distributed in all directions according to corresponding phase functions. A standard desert aerosol model [20] with a scale height of 1 km and a horizontal attenuation length of 25 km is assumed in the simulation. A ray-tracing procedure is carried out to trace each photon to the photo-cathodes of PMTs once the photons are generated. All detector responses are considered in the ray-tracing procedure. A detailed description of the ray-tracing procedure can be found in [21] and references therein. In figure 3, profiles of all kinds of photons that

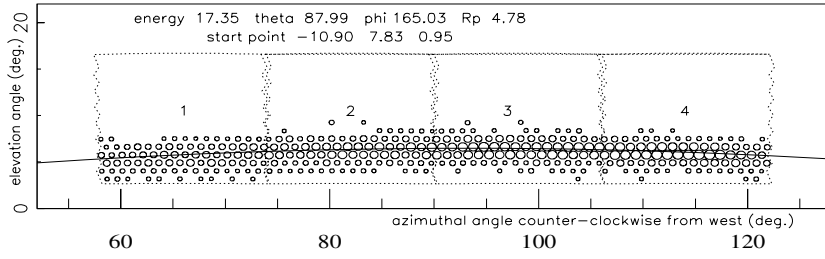


Figure 4. A typical horizontal air shower seen by the CRTNT detector. Each square marked with a number shows the FOV of each telescope. The circles represent triggered tubes and the size of each circle is proportional to the logarithm of the number of photons. The solid line represents a plane containing the shower axis and the detector. The energy (in PeV), zenith and azimuth angle (in degree), impact parameter and coordinates of the shower starting point (in km) are displayed.

are collected by the CRTNT detector are plotted as functions of the slant atmospheric depth along the shower longitudinal development for a typical simulated shower.

All photons collected by one PMT form a complete waveform according to their arrival time. Night sky background (NSB) photons with a flux of 40 photons per microsecond per square meter of the light collector are randomly added to the waveform. The electronic noise with a mean of 1.2 FADC counts per 20 ns is also added to every channel. A triggering algorithm at three levels as described in section 2 is implemented in the simulation. In figure 4, an example of a neutrino-induced shower event detected by the CRTNT is plotted.

3.4. Cosmic ray background simulation

As a background, CR showers are simulated with the core location being uniformly distributed in an area of $32 \text{ km} \times 10 \text{ km}$ between the mountain and detectors. CR shower energies are randomly selected from a spectrum of E^{-3} between 3 PeV and 1 EeV. All showers are between 70° and 75° in the zenith angle and between 0° and 180° in the azimuth angle. Cosmic rays from smaller zenith angles ($\theta < 70^\circ$) can be rejected according to their reconstructed geometry without any ambiguity. CRs from larger zenith angles ($\theta > 75^\circ$) are screened by the mountain.

Using Corsika (version 6.611), a shower library similar to that in neutrino simulation at 26 selected energies distributed from 3 PeV to 1 EeV and zenith angle at 75° is established. At each energy, 100 hadronic showers with the proton as primary particles are produced.

In the simulation, cosmic ray showers are randomly selected from the shower library. The slant atmospheric depth with an earth curvature correction, photon production, light propagation and trigger algorithm is the same as that used in the neutrino simulation. A uniform mountain profile with a height of 2.5 km is assumed to be 8 km away from the detectors serving as a screen.

4. Estimation of the event rate

Using the algorithm described in section 3, a ν_τ -to-shower conversion efficiency of 1.92×10^{-4} is yielded. An average trigger efficiency of showers induced by the products of τ decay is found to be approximately 21.8%. The input and observed event distribution are shown in figure 5. By using the AGN neutrino flux proposed by Semikoz and Sigl [9], the event rate is 35.7 per year assuming a duty cycle of 15% for the CRTNT detector. Although this AGN flux

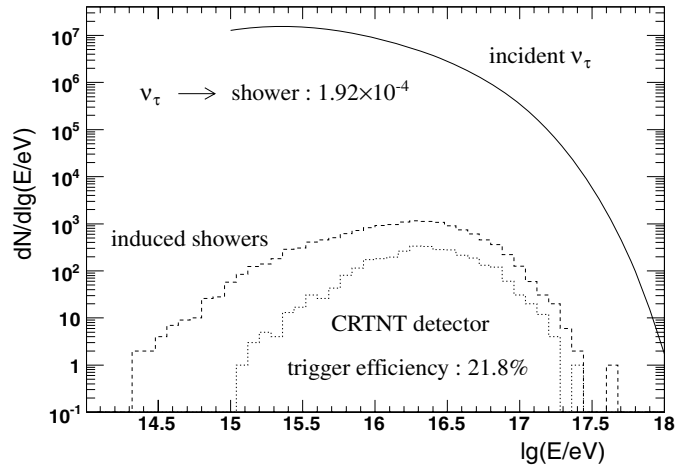


Figure 5. Input and observed event distribution using the CRTNT array in Mt Balikpapan. The solid curve represents the incident neutrino spectrum, the dashed curve is the induced shower energy distribution and the dotted curve shows the triggered events' energy distribution.

model was ruled out by the AMANDA experiment [22] we still use it for comparison with our previous study [7], where the same model was used.

We also estimate the event rates of the other two AGN models. The ν_τ -to- τ conversion efficiency of the MPR AGN jet model [10] is 2.14×10^{-4} . The triggering efficiency is 23.5%. The expected event rate is 27.3 per year. For an SDSS AGN core model [11, 12], the ν_τ -to- τ conversion and triggering efficiency are 7.25×10^{-5} and 12.5%, respectively. The expected event rate is 5.9 per year for this model.

The event rate of CR showers is estimated using the average flux $J(E) = 2 \times 10^{24} \times E^3 (\text{eV}^2 \text{ m}^{-2} \text{ s}^{-1} \text{ sr}^{-1})$ [23]. The trigger efficiency is found to be about 0.29% for CR showers. The input and observed spectra are shown in figure 6. In the simulation corresponding to an exposure of more than 2 years, 93 407 CR events are collected, i.e. 38 300.7 events will be detected per year.

5. Event selection

Neutrinos and CRs produce showers with distinct characteristics because they come from different directions and develop in different depths of the atmosphere. Without detailed shower reconstruction, a simple algorithm can identify neutrino events from CR background events by sorting potential neutrino events into the following five types.

- (i) *Up-going event.* A shower detector plane (SDP) is defined as a plane that contains the shower axis and the detector. An apparent up-going event, caused by neutrinos, can be identified by finding the elevation angles of triggered tubes along the SDP increasing with time. By checking the shower flying direction, a cut criterion in the time difference between the highest and the lowest tubes, denoted as dt , will pick out majority of neutrino events (41.5%). The dt distributions for apparent up-going neutrino ($dt > 0$) and all CR showers are shown in figure 7(a). In order to avoid cosmic ray showers that apparently go upward, a cut at 200 ns is chosen.

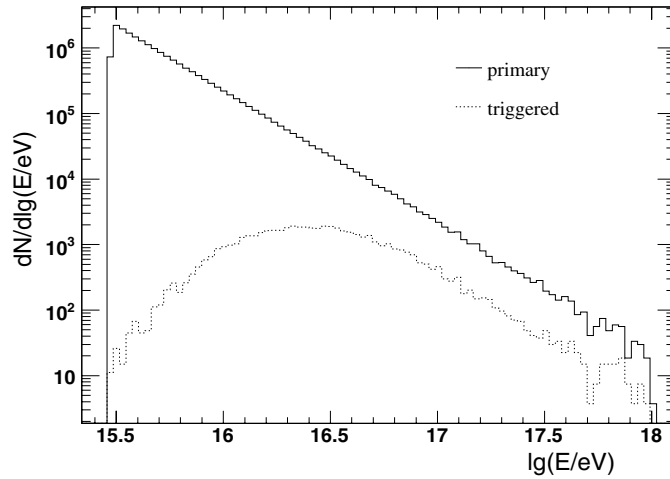


Figure 6. Energy distribution of primary CRs (solid curve) and triggered events (dashed curve).

- (ii) *Horizontal event.* An event whose SDP normal vector lies within a cone of 5° from the zenith is called a horizontal event. Such events might not be picked up as neutrino events by timing (i). The space angle between the SDP normal vector and the zenith, denoted as ψ , distributes as in figure 7(b). After the above step s^{-1} (the same in the following), approximately 7.9% of neutrino events are of this type. No cosmic rays belong to this category.
- (iii) *Neutrino-induced Cherenkov event.* Head-on showers generate Cherenkov images concentrating in an ellipse-like pattern. Because all photons arrive at the detector almost at the same time, the timing criterion does not work for this type of events. However, a neutrino-induced Cherenkov event must have the elevation angle of the center of image (COM), defined as a mean position weighted by triggered PMT signals, lower than 11° , because they come out from the mountain. CR events from such low directions start at very far away and are blocked by mountains. Only a small portion of them which just fly over the tip of the mountain may generate similar patterns, but the COMs must be at high positions. Figure 7(c) shows distributions of elevations of the COMs for different showers. A cut at 11° makes a clear separation between them. Approximately 17.7% of neutrino events belong to this category.
- (iv) *Very long track event.* Once an energetic shower starts at outside the FOV of the detectors, their shower tracks could be observed by multiple mirrors at one site as a characteristic. If it is induced by a mountain-passing neutrino, it is once again characterized by its low elevation of the COM. Therefore, cutting on both COM elevation and number of rows of triggered tubes in a shower as shown in figure 7(d), i.e. the COM elevation must be lower than 10° and the number of rows must be less than 13, neutrino events will be picked out. Only 7.2% events among all neutrino events belong to this category.
- (v) *Back-to-mountain event.* There must be some events with very clear characteristics that the first triggered tube located in the central area of the FOV of a telescope thus strongly indicates that τ leptons come out from the mountain and initiate a shower starting from where the tube points at. Without much effort, these neutrino events should be picked out if shower images start from points that are certainly not associated with any edges of the FOV. CR shower images must be engaged with the edges because the FOV is screened by

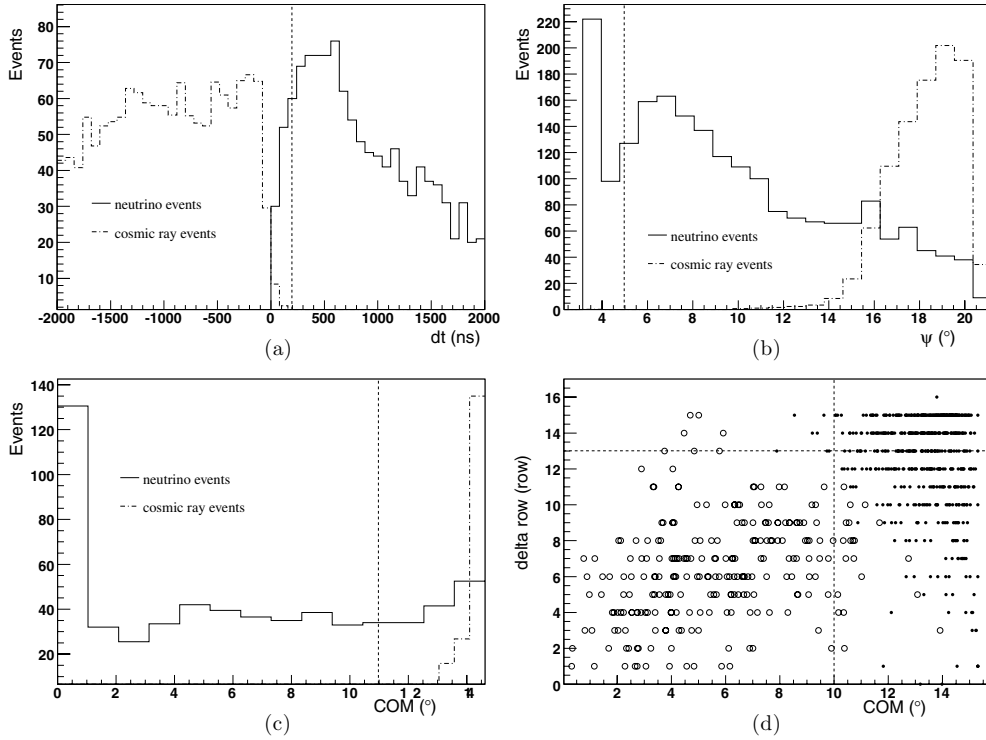


Figure 7. The distribution of parameters for neutrino-induced events (solid curves in (a)–(c) and open circle in (d)) and cosmic-ray-induced events (dash-dotted curves in (a)–(c) and solid circle in (d)). The dashed lines represent the cut criteria. (a) Average flying time for a shower over the FOV of the CRTNT detector. (b) The distribution of the space angle between the SDP normal vector and zenith. (c) COM elevation distribution for the Cherenkov events. (d) Number of rows of shower images versus the elevation of the center of image for very long track events. (See text for more details.)

the mountain. As a quantitative criterion, a FOV of 4° along the SDP between the starting point of an image and one of the edges is applied to select this type of events. This takes the reconstruction error of the SDP into account. However, only 5.8% of neutrino events fall in this category.

Summing them up, 80.1% of neutrino showers can be identified. The event rate for the AGN [9] reduces to 28.6 per year. The event rates for the MPR AGN jet model and SDSS AGN core model are 21.9 and 4.7 per year, respectively.

To estimate how many CR showers are mis-identified as neutrino events, we apply the proposed event selection algorithm to 93 407 CR events, and only one of them is selected as a neutrino event. This yields an average CR background of 0.4 event per year for the neutrino detection.

6. Sensitivity

We estimate the sensitivity of the CRTNT project using a modified Feldman–Cousins method [24]. The survival probability of the triggered neutrino events, defined as the number of

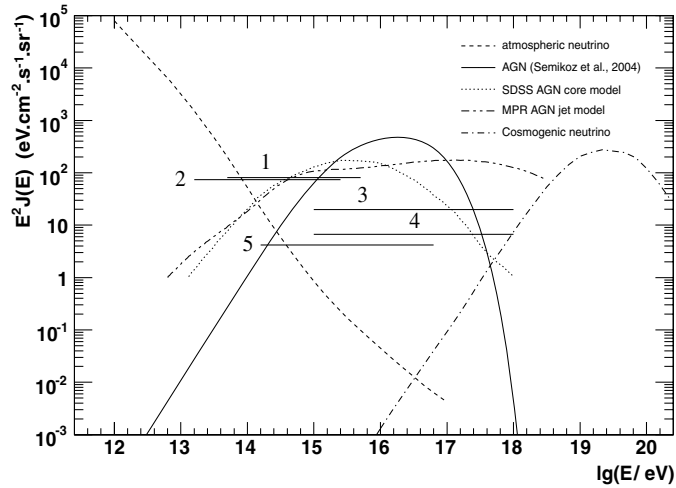


Figure 8. Predicted diffuse neutrino fluxes and sensitivities of the CRTNT project (horizontal solid lines) for tau neutrinos and other three experiments for muon neutrinos. The lines marked with numbers represent the upper limit of different experiments. Lines 3 and 4 are for CRTNT with 1 year and 3 year of observations, respectively. Line 1 is for Antares in one year of observation [26]. Line 2 is for Amanda II within 807 days of observation [22]. Line 5 is for IceCube with 3 years of observation [27].

Table 1. Optimization procedure of neutrino event selection.

$R(\%)^a$	n_s^b	$\langle n_b \rangle^c$	$\overline{\mu}_{90}^d$	Upper limit ^e
67.4	11.73	0.00	2.44	20.8
80.1	13.94	0.41	2.78	19.9
85.3	14.84	0.80	3.03	20.4
92.0	16.08	1.23	3.46	21.5

^a R is the neutrino event survival probability.

^b n_s represents the expected number of events per year from the model of Φ_s after the event selection.

^c $\langle n_b \rangle$ is the corresponding number of background cosmic ray events per year.

^d $\overline{\mu}_{90}$ shows the average upper limit from the Feldman–Cousins method [25].

^e The upper limit is in unit of $\text{eV cm}^{-2} \text{s}^{-1} \text{sr}^{-1}$.

identified neutrino events out of the total, is used as a reference parameter in the optimization procedure. By tuning the criteria, the survival probability changes from 67% to 92% as listed in table 1. The minimum upper limit goes to 19.9 ($\text{eV cm}^{-2} \text{s}^{-1} \text{sr}^{-1}$) with a hypothetical neutrino flux $\Phi_s = E^2 \cdot J(E) = 10^2 (\text{eV cm}^{-2} \text{s}^{-1} \text{sr}^{-1})$ with energies from 10^{15} to 10^{18} eV.

As a result, if no excess is observed in 1 year, an upper limit of 19.9 ($\text{eV cm}^{-2} \text{s}^{-1} \text{sr}^{-1}$) can be set with 90% C.L. by the CRTNT experiment. It falls to 6.7 ($\text{eV cm}^{-2} \text{s}^{-1} \text{sr}^{-1}$) for 3 years of observation. Figure 8 shows the corresponding results compared with other experiments. As references, three neutrino source models together with atmospheric and cosmogenic neutrino models are plotted in the same figure as well.

7. Conclusions

A complete simulation chain is developed including neutrino interaction, τ lepton decay, air shower and light production, detector responses, triggering and neutrino event selection algorithm. The event rate for a proposed AGN neutrino flux [9] is found to be 28.6 per year. The event rates for the MPR AGN jet model and SDSS AGN core model are 21.9 and 4.7, respectively.

Comparing with our previous estimate for the Mt Wheeler site [7], the expected annual event rate increases from 8 for three sites at the Mt Wheeler Peak to 28.6 for four sites at the Mt Balikun site according to the same AGN model. A significant improvement comes from (1) a much larger FOV of the CRTNT detector array at the Mt Balikun site because the mountain stretches longer with a height of about 4 km a.s.l., (2) an improvement of the detector design by widening the bandwidth of the light signals which are composed mainly of scattered Cherenkov light distributing over a range up to 600 nm and (3) a correction of an error in the previous simulation code about the Rayleigh scattering of Cherenkov photons which caused an underestimation of shower trigger efficiency by a factor of 2.5. The overall effect is about an enhancement of the event rate by a factor of 4.5. Other improvements have been made in the simulation by using a more detailed description about the neutrino interaction, τ lepton propagation in the mountain and its decay. Air shower generation is also improved as well.

According to a parametrization of CR event distribution, isotropic cosmic rays yield a background of 38 300.7 events per year in a zenith angle ranging from 70° to 75° . By using the neutrino event selection algorithm, 80.1% of 35.7 neutrino events with 0.4 CR background event per year are picked out. If the CRTNT does not see any signal excess within 1 year of observation, an upper limit of $19.9 \text{ (eV cm}^{-2} \text{ s}^{-1} \text{ sr}^{-1})$ with 90% C.L. can be concluded.

Acknowledgments

This work and the CRTNT project is supported by the Innovation fund (U-526) of the Institute of High Energy Physics (IHEP) and Hundred Talents & Outstanding Young Scientists Abroad Program (U-610/112901560333) from IHEP and Chinese Academy of Sciences. Authors MAH and TCL are supported by the National Science Council of Taiwan under project numbers NSC-95-2112-M239-003 and NSC-96-2112-M239-001.

References

- [1] Learned J G and Mannheim K 2000 *Annu. Rev. Nucl. Part. Sci.* **50** 679
- [2] Waxman E 2003 *Nucl. Phys. (Proc. Suppl.) B* **118** 353
- [3] Walter M (IceCube Collaboration) 2007 *Nucl. Phys. (Proc. Suppl.) B* **172** 13–6
- [4] Anton G (Antares Collaboration) 2005 *Nucl. Phys. (Proc. Suppl.) B* **143** 351–4
- [5] Abbasi R U *et al* (HiRes Collaboration) 2008 arXiv:0803.0554
- [6] Aramo C *et al* (Auger Collaboration) 2005 *Astropart. Phys.* **23** 65–77
- [7] Cao Z, Huang M A and Sokolsky P 2005 *J. Phys. G: Nucl. Part. Phys.* **31** 571–82
- [8] Aielli G *et al* (ARGO Collaboration) 2006 *Nucl. Instrum. Method Phys. Res. A* **562** 92
- [9] Semikoz D and Sigl G 2004 *J. Cosmol. Astropart. Phys.* **JCAP04(2004)003**
- [10] Mannheim K, Protheroe R J and Rachen J P 2000 *Phys. Rev. D* **63** 023003
- [11] Stecker F W, Done C, Salamon M H and Sommers P 1992 *Phys. Rev. Lett.* **69** 2738
- [12] Stecker F W 2005 *Phys. Rev. D* **72** 107301
- [13] Pumplin J *et al* 2002 *J. High Energy Phys.* **JHEP07(2002)012**
- [14] Ingelman G, Edin A and Rathsman J 1997 *Comput. Phys. Commun.* **101** 108–34 (LEPTO web page <http://www3.tsl.uu.se/thepl/lepto>)
- [15] Huang M A 2008 *Nucl. Phys. (Proc. Suppl.) B* **175-176** 472–5

- [16] Decker R *et al* 1993 *Comp. Phys. Commun.* **76** 361
Decker R *et al* 1992 *Comp. Phys. Commun.* **70** 69
Decker R *et al* 1990 *Comp. Phys. Commun.* **64** 275
Golonka P *et al* 2003 *Updates of TAUOLA CERN-TH 2003-287* arXiv:[hep-ph/0312240](https://arxiv.org/abs/hep-ph/0312240)
- [17] Heck D, Knapp J and Capdevielle J N 1998 *FZKA-6019, Institute fur Kernphys., University of Karlsruhe*
- [18] Krueger A J and Minzner R A 1976 *J. Geophys. Res.* **81** 4477–81
- [19] Kamata K and Nishimura J 1958 *Prog. Theor. Phys. Suppl.* **6** 93–100
- [20] Longtin D R 1998 *A Wind Dependent Desert Aerosol Model: Radiative Properties* Air Force Geophysics Laboratory, AFL-TR-88-0112
- [21] Abu-Zayyad T *et al* 2001 *Astropart. Phys.* **16** 1–11
- [22] Achterberg A *et al* (AMANDA Collaboration) 2007 *Phys. Rev. D* **76** 042008
- [23] Abu-Zayyad T, Belov K and Bird D J 2001 *Astrophys. J.* **557** 686–99
- [24] Hill G C and Rawlins K 2003 *Astropart. Phys.* **19** 393–402
- [25] Feldman G J and Cousins D R 1998 *Phys. Rev. D* **57** 3873–89
- [26] Montaruli T *et al* (Antares Collaboration) 2005 *Acta Phys. Polon. B* **36** 509–18 (arXiv:[hepex/0410079](https://arxiv.org/abs/hepex/0410079))
- [27] Ahrens J *et al* (IceCube Collaboration) 2004 *Astropart. Phys.* **20** 507–32